sustainability

MDPI

Article

Spatial–Temporal Restructuring of Regional Landscape Patterns and Associated Carbon Effects: Evidence from Xiong'an New Area

Yi-Hang Gao [1,2,3,4,†], Bo Han [1,2,3,4,*,†], Hong-Wei Liu [1,2,3,4,*], Yao-Nan Bai [1,2,3,4] and Zhuang Li [1,2,3,4]

[1] Tianjin Center, China Geological Survey, No. 4 Dazhigu 8th Road, Tianjin 300170, China; gaoyihang1988@163.com (Y.-H.G.); byaonan@mail.cgs.gov.cn (Y.-N.B.); lizhuang01@mail.cgs.gov.cn (Z.L.)
[2] North China Center of Geoscience Innovation, Tianjin 300170, China
[3] Xiong'an Urban Geological Research Center, China Geological Survey, No. 4 Dazhigu 8th Road, Tianjin 300170, China
[4] Tianjin Key Laboratory of Coast Geological Processes and Environmental Safety, No. 4 Dazhigu 8th Road, Tianjin 300170, China
* Correspondence: hanbo1984@126.com (B.H.); liuhenry022@163.com (H.-W.L.)
† These authors contributed equally to this work.

Abstract

China's accelerated urbanization has instigated construction land expansion and ecological land attrition, aggravating the carbon emission disequilibrium. Notably, the "land carbon emission elasticity coefficient" in urban agglomerations far exceeds international benchmarks, underscoring the contradiction between spatial expansion and low-carbon goals. Existing research predominantly centers on single-spatial-type or static-model analyses, lacking cross-scale mechanism exploration, policy heterogeneity consideration, and differentiated carbon metabolism assessment across functional spaces. This study takes Xiong'an New Area as a case, delineating the spatiotemporal evolution of land use and carbon emissions during 2017–2023. Construction land expanded by 26.8%, propelling an 11-fold escalation in carbon emissions, while emission intensity decreased by 11.4% due to energy efficiency improvements and renewable energy adoption. Cultivated land reduction (31.8%) caused a 73.4% decline in agricultural emissions, and ecological land network restructuring (65.3% forest expansion and wetland restoration) significantly enhanced carbon sequestration. This research validates a governance paradigm prioritizing "structural optimization" over "scale expansion"—synergizing construction land intensification with ecological restoration to decelerate emission growth and strengthen carbon sink systems.

Keywords: Xiong'an New Area; territorial space; carbon emission response

check for updates

Academic Editors: Yong Xiao, Jinlong Zhou, Qichen Hao, Wanjun Jiang and Jibin Han

Received: 23 May 2025
Revised: 3 July 2025
Accepted: 5 July 2025
Published: 7 July 2025

Citation: Gao, Y.-H.; Han, B.; Liu, H.-W.; Bai, Y.-N.; Li, Z. Spatial–Temporal Restructuring of Regional Landscape Patterns and Associated Carbon Effects: Evidence from Xiong'an New Area. *Sustainability* **2025**, *17*, 6224. https://doi.org/10.3390/su17136224

Copyright: © 2025 by the authors. Licensee MDPI, Basel, Switzerland. This article is an open access article distributed under the terms and conditions of the Creative Commons Attribution (CC BY) license (https://creativecommons.org/licenses/by/4.0/).

1. Introduction

Under the dual pressures of global climate change and the carbon neutrality transition, the spatiotemporal evolution of territorial spatial patterns has emerged as a core research topic in the sustainable development of human–environment coupled systems. Over the last three decades, global urbanization rates have surged from 43% to 57% [1]. China, as one of the fastest-urbanizing nations, has witnessed a 2.5-fold expansion of construction land, directly contributing nearly one quarter of the global increment in urbanization-related carbon emissions [2]. Concurrently, the shrinkage of ecological space, the non-grain conversion of cultivated land, and intensifying land use conflicts have systematically disrupted the carbon source–sink balance in territorial spaces. As per the IPCC assessment,

land use changes account for 23% of global carbon emissions [3]. China's rapid urbanization has resulted in a "land carbon emission elasticity coefficient" (defined as the ratio of the carbon emission growth rate to the construction land expansion rate) reaching 0.68, significantly surpassing the average levels for developed countries [4,5]. This phenomenon, most acutely manifested in urban agglomerations such as Beijing–Tianjin–Hebei and the Yangtze River Delta, reveals deep-seated contradictions between disordered territorial spatial expansion and low-carbon objectives [6–10].

Currently, research on the relationship between territorial space and carbon emissions has evolved toward an interdisciplinary perspective internationally. For instance, Zhangcai Qin et al. [11] utilized high-resolution satellite data, integrating remote sensing inversion, ground-based carbon flux observations, and Bayesian model uncertainty analysis, to achieve the first 1 km-resolution dynamic simulation of global land use carbon emissions. Their work reconstructed a 60-year spatiotemporal atlas of carbon emissions from global land use changes, quantifying the carbon contributions of deforestation, agricultural expansion, and urbanization. D. Rokityanskiy et al. [12] combined the IPCC carbon budget database with a Global Land System Multi-Agent Model (GLMAB) to develop a global-scale land use/carbon sink synergy model, simulating the carbon offset effects of bioenergy development and nature reserves under different climate scenarios (SSP1-5).

The advancement of China's "Dual-Carbon" strategy has positioned territorial space governance at the forefront in synergizing "carbon sink enhancement" and "emission control." The 2020 National Territorial Space Planning Outline explicitly proposed "guiding carbon emission reduction through spatial structure optimization," marking a transition from traditional land management paradigms to "carbon-constrained" governance. Studies by Guo Yi et al. [13] and Zhang Shuai et al. [14] revealed the carbon emission effects driven by policy interventions and land use adjustments in China's Yangtze River Delta region, along with their spatial heterogeneity, dynamic responses, and potential synergies with ecological conservation.

However, the existing research still faces several limitations, as follows: (1) Insufficient cross-scale mechanistic analysis: Most models (e.g., CLUE-S, InVEST) focus on single spatial categories or static scenario simulations, failing to capture the synergistic or antagonistic effects of "urban expansion–agricultural intensification–ecological restoration" at urban agglomeration scales [15,16]. (2) Underestimated spatiotemporal heterogeneity of policy impacts: For example, while the ecological conservation redline policy can curb carbon emission growth, its effectiveness varies significantly between Eastern developed regions and Western ecologically fragile areas [17,18]. (3) The limited localization of international experiences: The applicability of Europe's "compact city" theory to carbon reduction in China's high-density urban agglomerations remains contentious, while Japan's "garden city" model shows distinct carbon metabolic pathways compared to China's urban–rural integration practices [19]. (4) An inadequate understanding of spatial heterogeneity: Most models treat carbon emissions as homogeneous processes, overlooking the divergent carbon metabolic pathways across functional spaces such as urban agglomerations, ecological barrier zones, and agricultural production areas.

Therefore, taking the Xiongan New Area as a case study, this research employs a methodological framework integrating multi-stage dynamic analysis, the quantitative assessment of multi-type spatial interactions, the dynamic evaluation of policy responses, the analysis of policy implementation timing and effect lag, differentiated measurement across functional zones, and the heterogeneous analysis of carbon emission effects from spatial transformations. An in-depth analysis is conducted on the characteristics of land use changes since the New Area's establishment and the spatiotemporal evolution of carbon emissions induced by such changes. Specifically, this study aims to (1) support the

relocation of non-capital functions and efficient allocation of resources/elements in the Beijing–Tianjin–Hebei region through analyzing spatial pattern evolution and (2) provide empirical data for "dual-carbon" goal implementation by quantifying carbon emission effects. This research not only systematically addresses the gaps in the existing literature regarding cross-scale mechanism analysis, policy heterogeneity, the adaptation of international experiences to local contexts, and spatial disparity recognition but also offers transferable insights for optimizing territorial spatial configurations and achieving collaborative carbon emission governance in Chinese urban agglomerations.

2. Materials and Methods

2.1. Study Area

Xiong'an New Area is located in the North China Plain, within the hinterland triangle of Beijing, Tianjin, and Baoding. It encompasses Xiong County, Rongcheng County, Anxin County, and adjacent areas, covering a total area of 1770 km^2. With a population of 1.1197 million (2023), the region recorded a total GDP of CNY 41.27 billion, achieving a 19.42% year-on-year growth rate [20]. Geomorphologically situated at the eastern piedmont of the Taihang Mountains, the area belongs to an alluvial–proluvial plain [21]. The terrain exhibits remarkable flatness with ground slope gradients below 2‰. Climatically characterized as a warm temperate continental monsoon climate with semi-humid to semi-arid features, the region's environmental parameters are illustrated in Figure 1.

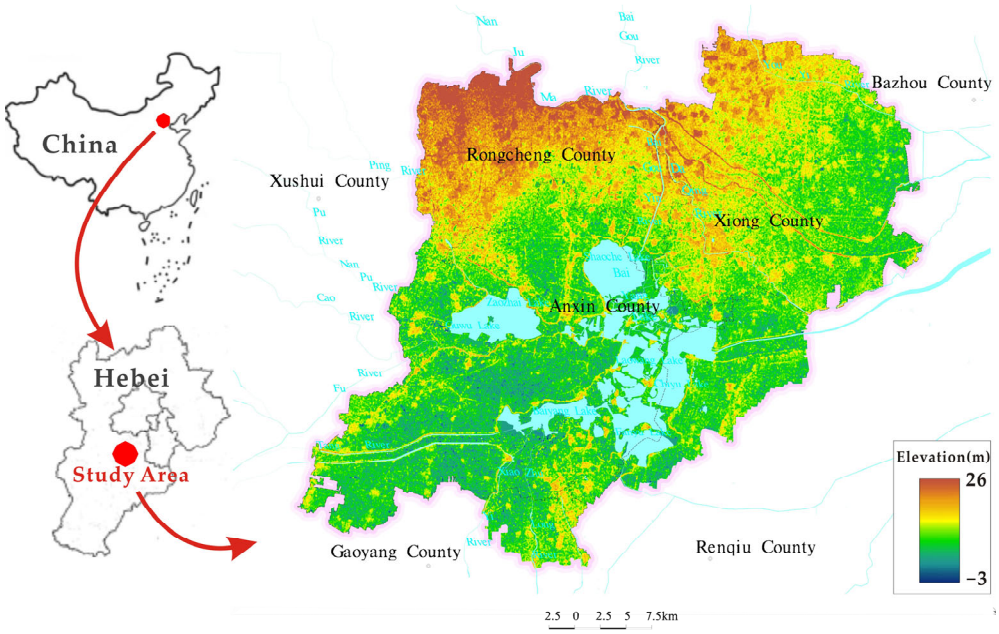

Figure 1. Schematic diagram of the geographical location of Xiongan New Area.

2.2. Data Sources

This study covers the period from 2017 to 2023, divided into four phases with a two-year interval. The four phases of Chinese land use data (2017, 2019, 2021, 2023) were derived from GF-2 satellite images with a 0.8 m resolution. These images were subject to visual interpretation in ENVI 5.3 software and validated through field surveys. The data used for carbon emission calculations (for the years 2017, 2019, 2021, and 2023) were obtained from the Baoding Economic Statistical Yearbook, Hebei Provincial Statistical Yearbook, Hebei Rural Statistical Yearbook, etc. The statistical data were aligned in space and time through grid allocation and temporal interpolation.

2.3. Land Spatial Classification System

This study adopts the National Ecological Remote Sensing Monitoring Land Use/Cover Classification System (NERM-LUCCS), integrating the Second National Land Survey baseline maps into the vegetation–soil composite classification framework developed by the Chinese Academy of Sciences. Building upon prior research achievements [22–24], we implemented an integrated approach combining manual visual interpretation techniques and field validation surveys. This methodology enabled the systematic acquisition of functionally differentiated land units in Xiong'an New Area, ultimately establishing a three-tier hierarchical spatial classification system. The framework delineates three primary spatial domains (agricultural, construction, and ecological) and six functionally distinct subcategories, agricultural production, residential development, forest, grassland, waterbody, and miscellaneous land covers, with detailed specifications provided in Table 1.

Table 1. Land space classification system for Xiongan New Area.

Land Use Function Classification		Secondary Classification of Land Use Classification System	Attribute
Primary Space	**Secondary Space**		
Agricultural Space	Agricultural Production Space	Paddy Fields, Dry Land	Carbon source/Carbon sink
Construction Space	Settlement Construction Space	Rural, Urban, and Transportation Land	Carbon source
Ecological Space	Forest Ecological Space	Forested Land, Shrub Land, Other Forested Land	Carbon sink
	Grassland Ecological Space	Artificial Grassland	Carbon sink
	Water Ecological Space	Rivers, Lakes, Pond, Marshlands	Carbon sink
	Other Ecological Space	Saline–Alkali land, Bare Land	Carbon sink

2.4. Transition Matrix

The transition matrix mathematically characterizes the spatiotemporal dynamics of land use transitions by describing linear transformations of initial probability vectors [24]. This stochastic operator quantifies state transition probabilities between discrete land categories, with its mathematical formulation expressed as follows:

$$S_{ij} = \begin{bmatrix} s_{11} & \cdots & s_{1n} \\ \vdots & & \vdots \\ s_{n1} & \cdots & s_{nn} \end{bmatrix} \quad (1)$$

where S is the land area; n is the number of types of land use; i, j are the types of land space utilization in the initial and final stages of the study, respectively; S_{ij} is the total area of the j-type land space at the end of the transition of the i-type land space at the beginning of the study. The transfer matrix can be visualized with the help of a Sankey diagram, which can more intuitively reflect the change in the transfer matrix (Yongxin LIU).

2.5. Carbon Emission Measurement of Land Use

Carbon emission measurement includes two approaches: the direct emission factor method and the indirect emission factor method. The direct emission factor method calculates emissions by multiplying a specific land area by its corresponding carbon emission factor, where a positive value indicates a carbon source and a negative value represents a carbon sink. In contrast, the indirect emission factor method applies when a direct calculation is infeasible due to complex human activity impacts (e.g., energy consump-

tion patterns). In such cases, emissions can be estimated indirectly using activity data parameters, such as energy consumption statistics.

In this paper, based on related research [25,26], we employ the direct carbon emission coefficient method to calculate carbon emissions for four types of ecological spaces: forest, grassland, water, and other ecological spaces, as well as carbon sink land spaces and agricultural production spaces with relatively fewer human activities. The calculation formula is as follows:

$$E_a = \sum e_i = \sum A_i \times \beta_i \quad (2)$$

where E_a represents the total carbon emissions (direct calculation value); e_i represents the carbon emissions of the i-th land use type; A_i is the area of the i-th land use type; and β_i is the carbon emission coefficient corresponding to the i-th land use type (Table 2) [27,28].

Table 2. Table of carbon emission coefficients for land use in Xiongan New Area (kg/m^2).

Land Use Type	Forest Ecological Space	Grassland Ecological Space	Water Ecological Space	Other Ecological Space	Agricultural Ecological Space
Carbon Emission Coefficient *	−0.0644	−0.021	−0.0257	−0.005	0.0422

* The positive value is the carbon source; the negative value is the carbon sink. Carbon emission coefficients are from references [27,28]. The research areas of this literature cover the Beijing–Tianjin–Hebei region and Hebei Province, which overlap with the study area of this paper. Therefore, these coefficients exhibit good applicability.

The carbon emissions from agricultural living spaces and urban construction spaces in the Xiongan New Area are indirectly calculated using the output values for secondary and tertiary industries and energy consumption per unit of GDP [29]. Specifically, taking the administrative division of the Xiongan New Area (three counties and surrounding areas) as the basic statistical unit, socio-economic data such as GDP and energy consumption (output values of secondary and tertiary industries) are statistically analyzed at the county level. The study area is then divided into 1 km × 1 km spatial grids, and county-level statistical data are allocated to each grid unit using the area-weighted method. The calculation formula is as follows:

$$Q_{i.j} = \frac{GDP_{2,3}}{A} \times a_{i,j} \quad (3)$$

$$E_{i,j} = Q_{i.j} \times H \times K \quad (4)$$

where $Q_{i.j}$ is the grid economic intensity; $GDP_{2,3}$ is the output value of secondary and tertiary industries at the county level; A is the total area of the county; $a_{i,j}$ is the area of the grid; $E_{i,j}$ is the grid carbon emissions (indirect calculation value); H is the energy consumption per unit of GDP; and K is the standard coal conversion factor.

3. Results

3.1. Analysis of Land Use Change Characteristics in Xiongan from 2017 to 2023

Figure 2 illustrates the spatial distribution of land use transitions in Xiongan New Area from 2017 to 2023, while Figure 3 depicts the quantitative changes in land use categories during the same period. Analysis of both figures reveals that land use changes in the area exhibit multi-scale and multi-dimensional characteristics, as outlined below:

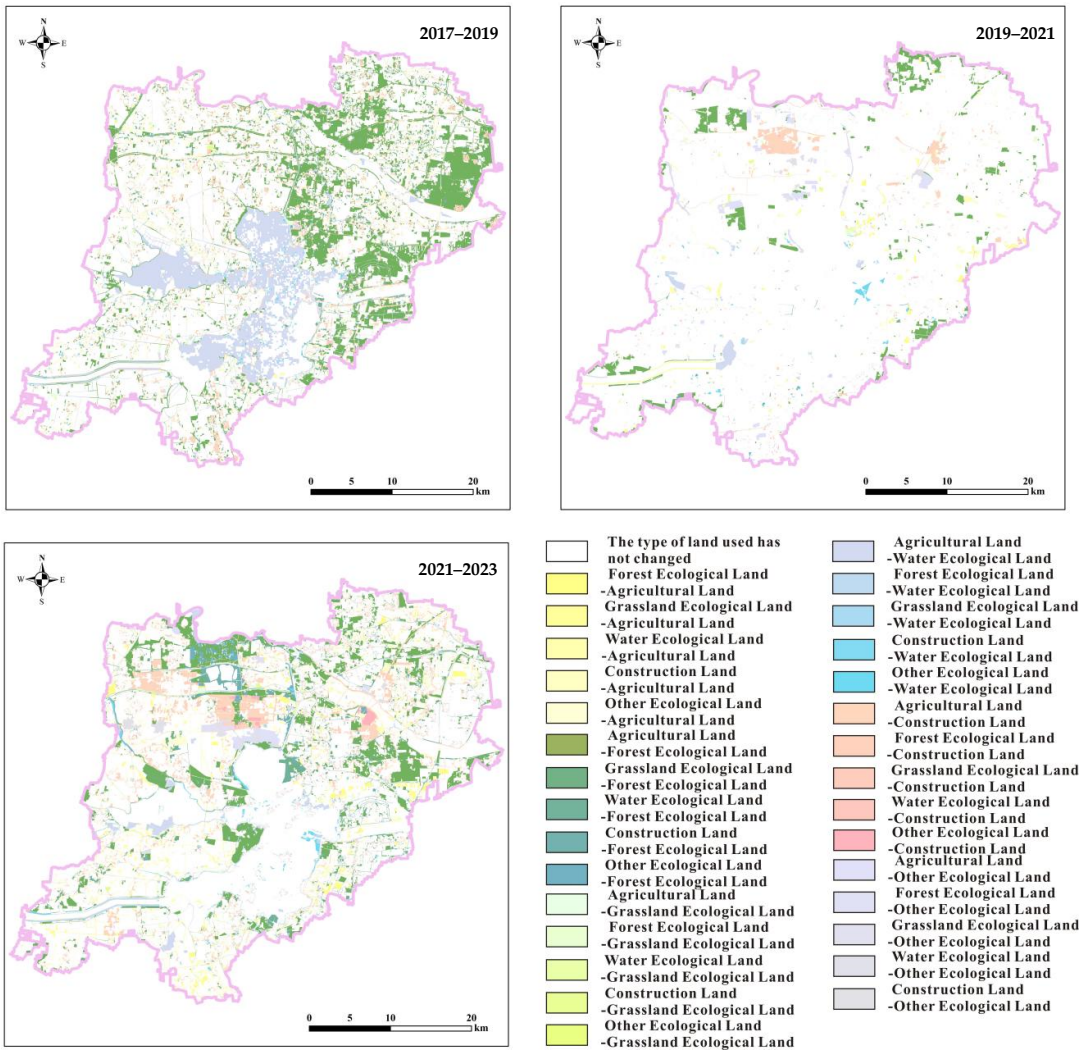

Figure 2. Spatial and temporal distribution of land use change in Xiongan New Area from 2017 to 2023.

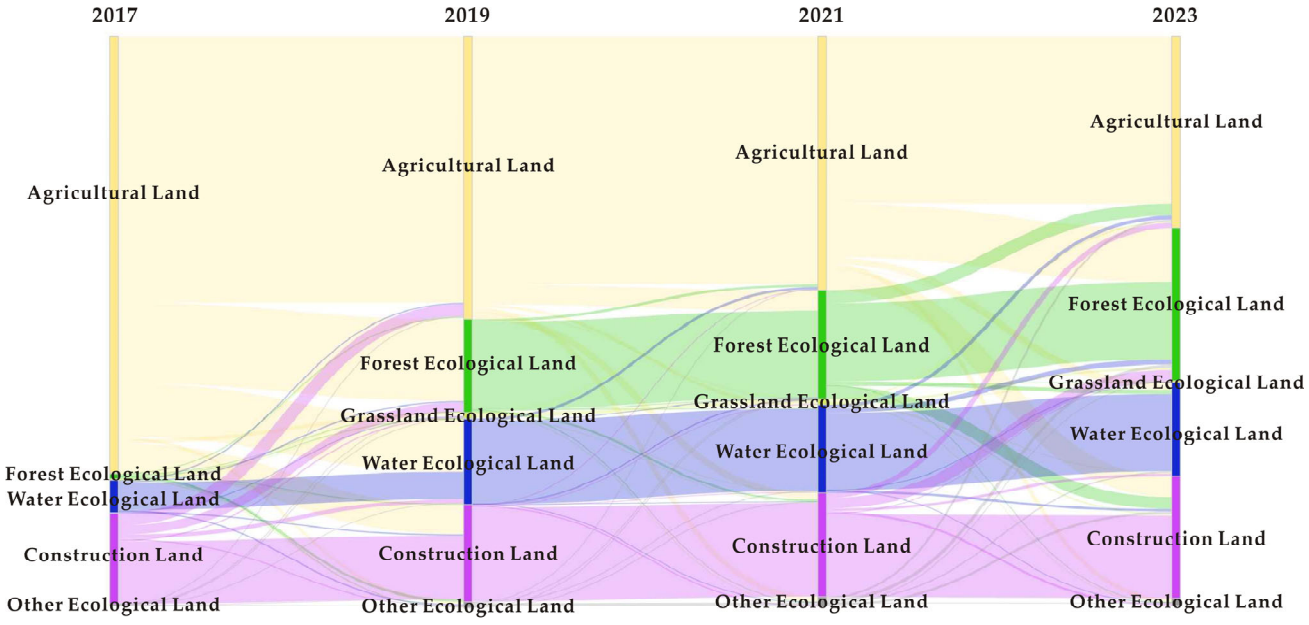

Figure 3. Land use change in Xiongan New Area from 2017 to 2023.

- The scale and structure of land use have undergone drastic adjustments. First, the rapid shrinkage of arable land is evident: the agricultural land area decreased from 876.54 km^2 in 2017 to 597.89 km^2 in 2023, representing a 31.80% decline. The period 2017–2019 witnessed the most rapid loss, with an average annual decrease of 41.5 km^2, primarily converted to construction land and water ecological land. Between 2019 and 2021, there was explosive growth, averaging an annual increase of 28.6 km^2. After 2021, the growth rate decelerated and shifted toward the construction of high-end industrial parks.
- The reconstruction of the ecological land network progressed in two primary aspects. Firstly, the quality of the forestland ecosystem was enhanced, with its area expanding from 287.5 km^2 to 475.14 km^2, primarily attributed to the "Millennium Xiulin" Project and the development of the urban green space system. Secondly, the restoration of the water wetland system achieved significant outcomes: the Baiyangdian Treatment Project maintained the water ecological land area within the range of 264–290 km^2, while the wetland area expanded to 366 km^2 (Table 3).

Table 3. List of differences in land use changes in Xiongan New Area from 2017 to 2023.

Stage	Characteristics	Land Use Change Magnitude
2017–2019	Infrastructure Initiation Phase	The agricultural land area decreased by 83 km^2, while the construction land area increased by 23 km^2
2019–2021	Functional Transition Phase	The construction land area increased by 56 km^2, while the ecological land area increased by 49 km^2
2021–2023	Industry–City Integration Phase	The construction land area increased by 27 km^2

To summarize, the characteristics of land use changes in Xiong'an New Area since its establishment have validated its planning philosophy of "global vision, international standards, Chinese characteristics, and high-tier positioning". Current land utilization has shifted from scale expansion to structural optimization, with the focus now on enhancing both GDP output per unit of land and carbon sink capacity.

3.2. Analysis of Spatial and Temporal Evolution Characteristics of Carbon Emissions in Xiongan from 2017 to 2023

Figure 4 shows the changes in carbon emissions in Xiongan New Area from 2017 to 2023, while Figure 5 illustrates the relationship between these changes and land use-related carbon emission intensity during the same period (the carbon emissions from construction land quantify the carbon output of human activities in "tons", while the carbon sink of ecological land quantifies the carbon absorption of natural systems in "negative tons". The two directly reflect the regional carbon balance at the total quantity level). It can be seen from the figure that the following is true:

- Construction land dominated the growth in total carbon emissions, which surged from 281 kt (kilotons) in 2017 to 3322 kt in 2023—a nearly 11-fold increase—with its share of regional total emissions rising from 3% to 87%. This surge was primarily driven by the expansion of the construction land area from 284.50 km^2 to 379.10 km^2, coupled with industrial aggregation. Notably, despite this substantial growth in emissions, the carbon emission intensity decreased from 988.58 t/km^2 to 876.31 t/km^2, attributable to energy efficiency improvements and renewable energy integration, as evidenced by Green Building Standards and Operational Energy Efficiency Gains—green building standards cut unit energy use by 28.7% (2021–2023 vs. 2017 baseline), with monitoring platforms reducing lighting/air conditioning energy consumption by

15–20%, lowering operational intensity from 1.25 to 0.89 t/m^2 (45% of decline)—and renewable energy integration and energy structure transformation—"BIPV + regional renewable energy stations" increased non-fossil energy in electricity (27–59% by 2023) and heating (12–78%), reducing intensity by 32% [30].

- Carbon emissions from cultivated land continued to shrink, declining from 94,740,000 tons to 25,230,000 tons (a 73.40% decrease). This reduction was directly linked to the contraction of cultivated area from 1380.60 km^2 to 597.90 km^2. However, the carbon emission intensity remained stable at 42,200 tons/km^2, indicating that the promotion of low-carbon agricultural technologies is insufficient and reliance on traditional farming models persists.
- The carbon sink capacity of ecological land has significantly improved. The carbon sink of the forest ecological space has increased from −1,375,000 tons to −30,601,000 tons, while its area has expanded from 0.22 km^2 to 475.16 km^2, thanks to the 'Millennium Show Forest' project. Additionally, due to the ecological restoration of Baiyangdian, the carbon sink of the water ecological space has stabilized at −4,190,000 to −7,420,000 tons.

(**a**)

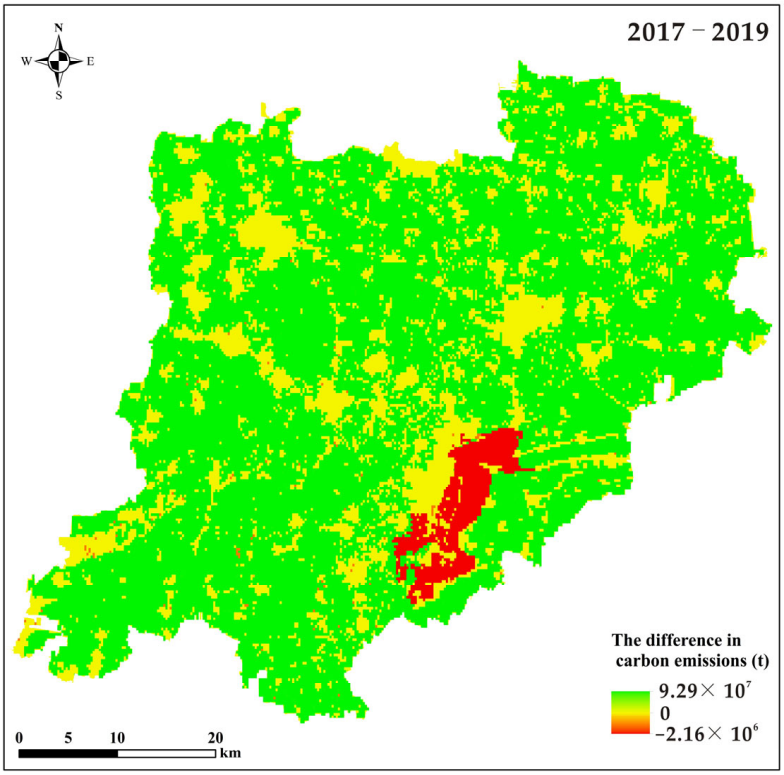

Figure 4. *Cont.*

(**b**)

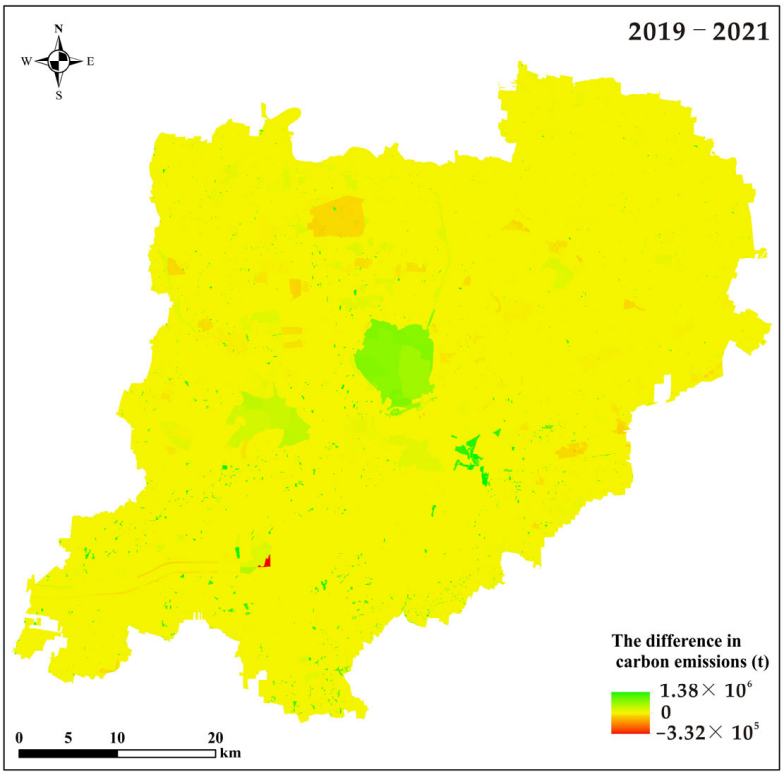

(**c**)

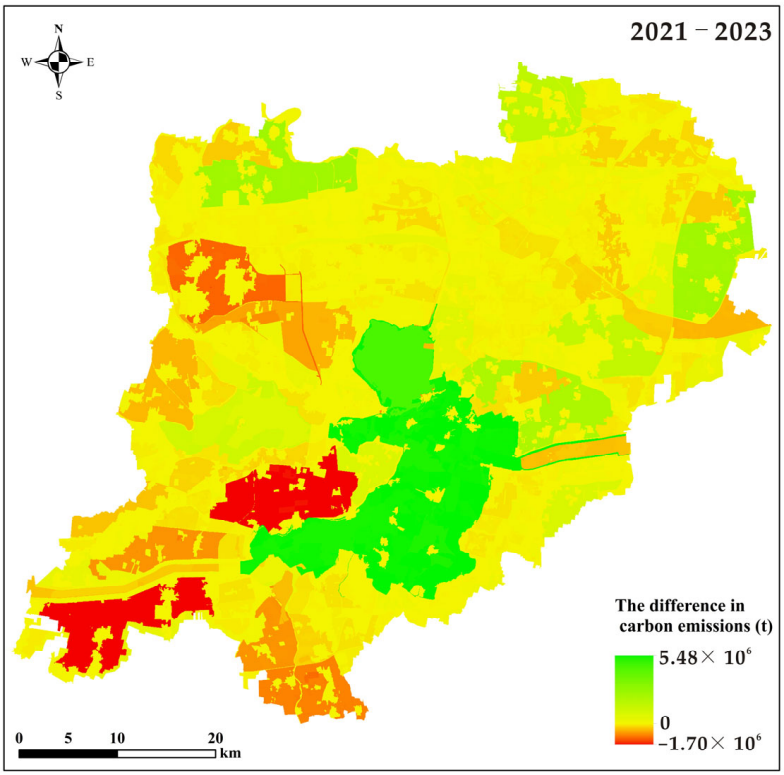

Figure 4. Schematic diagram of carbon emissions in Xiongan New Area from 2017 to 2023. The red in the figure represents an increase in carbon emissions, green represents a decrease in carbon emissions, and the shade of color indicates the intensity of change, reflecting the temporal correlation between each phase and carbon metabolism: (**a**) Infrastructure Initiation Phase, (**b**) Functional Transition Phase, (**c**) Industry–City Integration Phase.

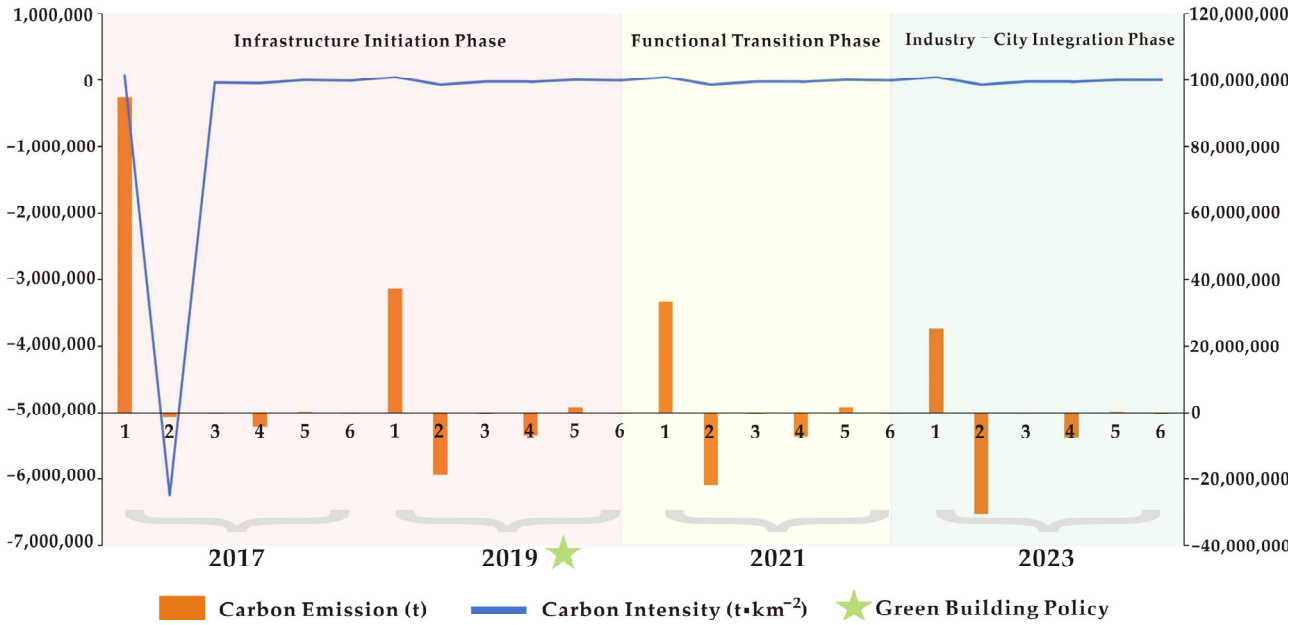

Figure 5. Schematic diagram of the relationship between land use carbon emissions and carbon emission intensity in Xiongan New Area from 2017 to 2023. 1 is Agricultural Land; 2 is Agricultural Land; 3 is Grassland Ecological Land; 4 is Water Ecological Land; 5 is Construction Land; and 6 is Other Ecological Land.

3.3. Analysis of Land Use Carbon Emission Effect

Human activities directly or indirectly alter carbon cycling processes in terrestrial ecosystems through changes in land cover types, utilization methods, and management practices. These modifications lead to shifts in atmospheric greenhouse gas balance, a phenomenon defined as the land use carbon effect. Table 4 demonstrates the evolution of land use patterns and associated carbon effects in Xiongan New Area during 2017–2023. The data reveal that since the establishment of this new development zone, carbon effects stemming from land use transformations have exhibited distinct phased characteristics.

- 2017–2019: Rapid rise in carbon emissions

This stage is the initial phase of the new area's establishment, during which the expansion of construction land dominated carbon emissions. The carbon effect from converting agricultural land to construction land reached −10.92 billion tons, which accounted for the dominant proportion of the total carbon emission effect. This reflects how rapid urbanization has led to land sealing, the rapid loss of soil carbon pools, and a short-term surge in carbon emission intensity. The conversion of land for ecological purposes showed initial negative effects. Specifically, the transformation of agricultural land into forestland or surface water ecological land exhibited significant negative carbon effects. Among these, the carbon effect of converting agricultural land to forest ecological land amounted to −7.56 billion tons, likely due to soil disturbance emissions during the early stages of vegetation restoration.

- 2019–2021: Carbon emission fluctuation adjustment period

Due to policy-driven interventions, the carbon effect of converting agricultural land to construction land has shifted from negative to positive. This shift may result from the large-scale adoption of green building technologies in Xiongan New Area or the integration of low-carbon infrastructure practices within construction land to partially offset emissions. Meanwhile, the carbon effect of converting other ecological land to construction land declined to −1.026 billion tons, reflecting the containment of sensitive land encroachment

through stricter ecological protection policies. At this stage, the carbon effect of converting construction land to forest or surface water ecological land remains negative at −0.06 billion tons, revealing a lag in ecological restoration processes. Such persistence suggests that high carbon costs are still incurred during initial restoration phases, likely due to soil carbon loss and ecosystem destabilization caused by land use transitions.

Table 4. Land use type change and carbon effect change in Xiongan New Area from 2017 to 2023.

Land Use Transition Type	Total Carbon Effect × 10^8 tons		
	2017–2019	2019–2021	2021–2023
Agricultural Land—Forest Ecological Land	−7561.2734	−0.1179	−25.2733
Agricultural Land—Grassland Ecological Land	−827.2535	−0.0014	−0.0127
Agricultural Land—Water Ecological Land	−1675.1332	−0.0370	−4.2645
Agricultural Land—Construction Land	−10,915.6132	0.0329	0.2918
Agricultural Land—Other Ecological Land	−0.3343	−0.8100	−0.1147
Forest Ecological Land—Agricultural Land	0.0344	0.0352	10.1504
Forest Ecological Land—Grassland Ecological Land	0.0023	0.0008	−0.0024
Forest Ecological Land—Water Ecological Land	−0.0241	−0.0151	−7.3916
Forest Ecological Land—Construction Land	0.0382	0.0678	0.7259
Forest Ecological Land—Other Ecological Land	0.8168	−0.2794	−0.0450
Grassland Ecological Land—Agricultural Land	0.0007	0.0035	1.8505
Grassland Ecological Land—Forest Ecological Land	−0.0007	−0.0004	−2.1806
Grassland Ecological Land—Water Ecological Land	−0.0444	−0.0006	−0.5154
Grassland Ecological Land—Construction Land	0.0003	0.0162	0.0414
Grassland Ecological Land—Other Ecological Land	0.0123	−0.0190	−0.0110
Water Ecological Land—Agricultural Land	0.7365	0.0124	3.2192
Water Ecological Land—Forest Ecological Land	1.1311	0.0011	−4.6886
Water Ecological Land—Grassland Ecological Land	0.1663	0.0000	−0.0003
Water Ecological Land—Construction Land	3.3591	0.0099	0.1331
Water Ecological Land—Other Ecological Land	0.6422	−0.0590	−0.0065
Construction Land—Agricultural Land	0.0443	0.0192	19.3326
Construction Land—Forest Ecological Land	−0.1949	−0.0061	−33.0676
Construction Land—Grassland Ecological Land	−0.0143	−0.0025	−0.0045
Construction Land—Water Ecological Land	−0.1357	−0.0238	−31.3456
Construction Land—Other Ecological Land	4.2442	−0.1855	−0.1141
Other Ecological Land—Agricultural Land	0.0077	−1.4059	1.0027
Other Ecological Land—Forest Ecological Land	−0.0015	−1.3571	−0.8140
Other Ecological Land—Grassland Ecological Land	0.0000	−0.1729	0.0129
Other Ecological Land—Water Ecological Land	−0.0046	−0.7193	0.1079
Other Ecological Land—Construction Land	0.0007	−10.2558	0.4486
Total	−20,968.7908	−15.2698	−72.5354

- 2021–2023: Carbon emission partial rebound period

At this stage, the conversion of construction land to forest or surface water ecological land exhibited a significantly deteriorated carbon effect, with emissions reaching −3.135 billion tons. This deterioration is likely linked to large-scale hydrological restoration projects disturbing subsoil carbon reservoirs during ecosystem reconstruction. Conversely, the conversion of forest land to agricultural use generated a sharply increased carbon effect of 1.015 billion tons, primarily driven by biomass depletion and accelerated soil carbon mineralization under land use intensification. Meanwhile, the carbon effect of converting agricultural land to construction land showed marked improvement, attributed to optimized urban green infrastructure offsetting partial emissions through enhanced vegetation

carbon sequestration. Additionally, the conversion of other ecological land to agricultural land resulted in a carbon effect of 0.1 billion tons, exhibiting positive fluctuations. This underscores the need to balance carbon sink conservation and land use efficiency when developing reserve land resources (Table 5).

Table 5. Land use type and carbon effect changes in Xiongan New Area from 2017 to 2023.

Phase	Key Drivers	Typical Carbon Effect Shifts	Implications
2017–2019 (Expansion Phase)	Rapid urbanization and ecological land encroachment	Construction land expansion dominates high carbon emissions	Strict control over development intensity must be enforced, prioritizing the protection of high-carbon-sink ecological land
2019–2021 (Adjustment Phase)	Green policy interventions and early stages	Carbon effect of construction land conversion shifts from negative to positive	Strengthening the application of low-carbon technologies in ecological restoration projects
2021–2023 (Rebound Phase)	Hidden emission from ecological engineering vs. reserve land development dilemmas	Surge in carbon emissions from conversion of construction land to ecological land	Optimizing the sequencing of land use transitions to avoid "carbon-for-carbon" remediation approaches

4. Conclusions

This study analyzed land use changes and their carbon effects in Xiong'an New Area from 2017 to 2023, yielding the following core findings:

- Transformation of Land Use Structure

Since its establishment, the construction land area in Xiongan New Area has increased by 26.8% (from 284.50 km^2 to 379.10 km^2), emerging as the dominant carbon emission source (with the proportion rising from 3% to 87%). Concurrently, the cultivated land area decreased by 31.8%, leading to a corresponding 73.4% decline in agricultural carbon emissions. Ecological land has expanded significantly: the forest area has increased by 65.3%, and wetland restoration has steadily enhanced the carbon sink capacity of aquatic ecological spaces.

- Dynamics and Stage-specific Characteristics of Carbon Emissions

Carbon emissions from construction land increased 11-fold, while the carbon emission intensity per unit area decreased by 11.4%, reflecting improved energy efficiency and the application of renewable energy technologies. The carbon sink capacity of forest ecological spaces increased from −1.375 million tons to −30.601 million tons. Ecological restoration projects (e.g., the "Millennium Xiulin" project) significantly enhanced the carbon absorption capacity. In 2017–2019 (Expansion Phase), carbon emissions grew rapidly, with the carbon effect of converting cultivated land to construction land accounting for 52.1% of total emissions. Initial ecological restoration was accompanied by carbon emissions from soil disturbance during vegetation establishment. In 2019–2021 (Adjustment Phase), green building policies shifted the carbon effect of construction land from net emission to partial neutralization. However, the lag in ecological restoration resulted in persistently high carbon costs due to delayed carbon sequestration. In 2021–2023 (Rebound Phase), ecological engineering interventions disturbed deep soil carbon pools, while the partial reclamation of cultivated land exacerbated fluctuations in carbon emissions.

5. Discussions

- The finding that "construction land expansion drives carbon emission growth" in this study aligns with Zou et al. (2025)'s research on urban agglomerations in the Yangtze River Delta, which demonstrated a positive correlation between urbanization rate and carbon emissions [31–33]. However, the carbon sink growth effect achieved through ecological restoration in Xiongan New Area (with forest coverage increasing by 65.3%) significantly exceeds the average level of Hebei Province. Luo et al. (2024) reported an average annual growth of 7.9% in ecological carbon sinks in this region [28], which may be directly attributed to the new area's planning strategy of "planting greenery before constructing the city". In terms of carbon emission intensity, this study reveals a 11.4% decrease in unit carbon emissions from construction land, consistent with the theory proposed by D. Rokityanskiy et al. (2007) that "compact cities can reduce energy consumption per unit area" [12]. Nevertheless, this decline remains lower than that observed in European "compact city" cases (e.g., Copenhagen's annual unit carbon emission reduction of 15–20%). This suggests that Xiongan New Area needs to further optimize its energy structure rather than relying solely on spatial intensification.
- The carbon coefficients employed in this study are derived from previous research [27,28], which may exhibit deviations from local data in Xiongan. In the future, it will be essential to establish a localized carbon accounting system by integrating remote sensing inversion and ground-based measurements (such as carbon flux observations in Baiyangdian Wetland). This approach aligns with the trend of the "high-resolution carbon simulation framework" proposed by Qin et al. (2024) [11]. Simultaneously, introducing the CLUE-S model to simulate multi-scenario land use transitions [15] can provide more accurate decision support for spatial planning under the "dual-carbon" goals.

Author Contributions: Conceptualization, Y.-H.G. and B.H.; methodology, Y.-H.G.; software, Y.-H.G.; validation, B.H., Y.-N.B., and Z.L.; formal analysis, Y.-H.G.; investigation, B.H., Y.-N.B., and Z.L.; resources, H.-W.L.; data curation, Y.-H.G.; writing—original draft preparation, Y.-H.G.; writing—review and editing, B.H.; visualization, Y.-H.G.; supervision, B.H.; project administration, H.-W.L.; funding acquisition, H.-W.L. All authors have read and agreed to the published version of the manuscript.

Funding: This research was funded by the Monitoring and Evaluation of Resource and Environment Carrying Capacity of the Beijing–Tianjin–Hebei Collaborative Development Area and Xiongan New Area (Grant no. DD20221727) and Detailed Investigation and Risk Control of Geological Disasters in Taihang Lvliang Mountain Area (Grant no. DD20230438).

Institutional Review Board Statement: Not applicable.

Informed Consent Statement: Not applicable.

Data Availability Statement: This study does not involve any patented technologies that have been applied for or are under review. All experimental data and methodologies were conducted in accordance with publicly available scientific research protocols.

Conflicts of Interest: The authors declare no conflicts of interest.

References

1. United Nations Human Settlements Programme (UN-Habitat). *World Cities Report 2022: Envisaging the Future of Cities*; UN-Habitat: Nairobi, Kenya, 2022.
2. Ye, X.; Chuai, X.W. Carbon sinks/sources' spatiotemporal evolution in China and its response to built-up land expansion. *J. Environ. Manag.* **2022**, *321*, 115863. [CrossRef] [PubMed]
3. IPCC. *Climate Change 2023: Synthesis Report. Contribution of Working Groups I, II and III to the Sixth Assessment Report of the Intergovernmental Panel on Climate Change*; IPCC: Geneva, Switzerland, 2023.

4. Zhao, D.; Li, T. Analysis of carbon emissions and the influence factors in the process of urbanization among Chinese Provinces. *Acta Sci. Nat. Univ. Pekin.* **2016**, *52*, 947–958.
5. Liu, J.; Wu, B.; Wang, H.; Wei, G. Spatial differentiation and dynamic analysis of land use change in China under different carbon emission scenarios. *Bull. Soil Water Conserv.* **2025**, *45*, 1–11.
6. Li, C.; Zhao, R.; Wang, F.; Wang, F.; Hu, Y.; Yang, P.; Zhao, Y. Current situation fo the coastal wetlands in Guangxi and analysis of carbon storage in the mangrove wetland. *North China Geol.* **2022**, *45*, 62–68.
7. Huang, L.; Li, L.; Wang, W. Research on comprehensive evaluation and regionalization of natural resources in North China based on GIS. *North China Geol.* **2023**, *46*, 83–88.
8. Liu, M.; Chen, Y.; Wang, J.; Chen, K.; Chen, Y. The spatial association network and driving factors of land use carbon emission efficiency in China: An investigation in the national major strategic regions. *Resour. Sci.* **2024**, *46*, 2462–2476.
9. Lv, Q.; Luo, Y.; Gao, Z.; Lei, X. Spatio-temporal pattern, dynamic evolution, and carbon compensation zoning of land use carbon budget in Beijing-Tianjin-Hebei Region. *Environ. Sci.* **2025**. [CrossRef]
10. Li, Z.; Xu, L.; Ye, Y.; Wu, Q. Spatiotemporal differentiation of carbon budget and carbon compensation zoning in the Yangtze River Delta Urban agglomeration. *Environ. Sci.* **2025**. [CrossRef]
11. Qin, Z.; Zhu, Y.; Canadel, G.; Chen, M.; Li, T.; Mishar, M.; Yuan, W. Global spatially explicit carbon emissions from land-use change over the past six decades (1961–2020). *One Earth* **2024**, *7*, 835–847. [CrossRef]
12. Rokityanskiy, D.; Benítez, P.; McCallum, I.; Obersteiner, M.; Rametsteiner, E.; Yamagata, Y. Geographically explicit global modeling of land-use change, carbon sequestration, and biomass supply. *Technol. Forecast. Soc. Change* **2007**, *74*, 1057–1082. [CrossRef]
13. Guo, Y.; Cao, X.; Wei, W.; Zeng, G. The impact of regional integration in the Yangtze River Delta on urban carbon emissions. *Geogr. Res.* **2022**, *41*, 181–192.
14. Zhang, S.; Yuan, C.; Zhao, X. Spatial and temporal characteristics of land use carbon emission intensity in the central area of Yangtze River Delta from 2000 to 2018. *J. Henan Agric. Univ.* **2019**, *39*, 122–129.
15. Bian, Z.; Ma, X.; Gong, L.; Zhao, J.; Zeng, C.; Wang, L. Land use prediction based on CLUE-S model under different Non-spatial simulation methods: A case study of the Qinhuai River watershed. *Sci. Geogr. Sin.* **2017**, *37*, 252–258.
16. Wei, L.; Zhou, L.; Sun, D.; Tang, X. The evolution of spatio-temporal pattern and scenario simulation of urban agglomeration expansion in the Yellow River Basin: A case study in the Hohhot-Baotou-Ordos-Yulin urban agglomeration. *Geogr. Res.* **2022**, *41*, 1610–1622.
17. Shi, D.; Shi, K. Analysis of the targets, stylized facts and influencing factors of green and low-carbon development in China: Based on a literature review. *Soc. Sci. Int.* **2023**, *4*, 95–120+243–244.
18. Tian, Y.; Cai, Y. EKC-based test for agricultural carbon emissions in Yangtze River economic belt and analysis of driving factors. *Resour. Environ. Yangtze Basin* **2023**, *32*, 2403–2417.
19. Xie, X.; Zhang, C. Research on Shanghai planning management strategy under the "carbon emissions peak and carbon neutrality": Based on analysis of international experiences. *Shanghai Urban Plan. Rev.* **2023**, *3*, 71–77.
20. Ma, Z.; Xia, Y.; Li, H.; Han, B.; Yu, X.; Zhou, Y.; Wang, Y.; Guo, X.; Li, H.; Pei, Y. Analysis of natural resources and environment eco-geological conditions in Xiong'an New Area. *Geol. China* **2021**, *48*, 677–696.
21. Han, B.; Xia, Y.; Ma, Z.; Wang, X.; Guo, X.; Lin, L.; Pei, Y. Division of engineering geological strata, building of 3D geological structure and its application in urban planning and construction in Xiong'an New Area. *Geol. China* **2023**, *50*, 1903–1918.
22. Lu, Z.; Zhang, Z. Research on regional variability in the evolution of territorial space pattern and its driving factors in Beijing-Tianjin-Hebei Region. *China Land Sci.* **2022**, *36*, 42–52.
23. Lin, J.; Liu, Q.; Li, J. Research on establishing a land space utilization classification for new urbanization. *Urban Stud.* **2016**, *23*, 51–60.
24. Lin, Y.; Zhao, J.; Zhang, M.; Chen, G. Identification of territory space pattern and spatio-temporal evolution analysis of urban agglomeration in central Yunnan. *Trans. Chin. Soc. Agric. Mach.* **2019**, *50*, 176–191.
25. Su, Y.; Zhang, Y. Study on effects of carbon emission by land use patterns of Shaanxi Province. *J. Soil Water Conserv.* **2011**, *25*, 152–156.
26. Lai, L.; Lv, W.; Shu, L. Discussion on the design of carbon pricing system with Chinese characteristics under dual-carbon goal. *New Financ.* **2022**, *5*, 45–52.
27. Li, A.; Yin, X.; Wei, H. Spatio-temporal evolution of carbon emission from land use and its driving factors in Beijing-Tianjin-Hebei districts and counties. *Environ. Sci.* **2024**, *44*, 2270–2283.
28. Luo, Y.; Chen, S.; Liu, W.; Wang, X.; Qi, A. Analysis and prediction on the spatiotemporal evolution of carbon emissions from land use in Hebei province. *Chin. J. Environ. Eng.* **2024**, *11*, 3360–3373.
29. Wang, G.; Nan, L. Temporal-spatial variance of carbon emission effect in Shaanxi's land use. *Resour. Ind.* **2012**, *14*, 124–130.
30. Hebei Xiong'an New Area Management Committee. *Guidelines for High-Quality Development of Green Building in the Xiong'an New Area*; Hebei Xiong'an New Area Management Committee: Baoding, China, 2021.

31. Zou, X.; Yang, L.; Sun, X.; Liu, S. Study on the measurement of peak carbon levels, spatial and temporal evolution, and influencing factors in the Yangtze River delta urban agglomeration. *Soft Sci.* **2025**. Available online: http://kns.cnki.net/kcms/detail/51.1268.G3.20250613.1846.002.html (accessed on 22 May 2025).
32. Li, Y.; Zhao, Q.; Lin, W.; Li, Y.; Liu, H.; Fang, Q. Spatial and temporal evolution of carbon emission and influencing factors in Yangtze River delta based on luminous remote sensing data. *J. Atmos. Environ. Opt.* **2024**. Available online: http://kns.cnki.net/kcms/detail/34.1298.O4.20240509.1131.002.html (accessed on 22 May 2025).
33. Feng, X.; Li, Y.; Yu, E.; Yang, J.; Wang, S.; Ma, J. Spatiotemporal pattern and coordinating development characteristics of carbon emission performance and land use intensity in the Yangtze River delta urban agglomeration. *Trans. Chin. Soc. Agric. Eng.* **2023**, *39*, 208–218.

Disclaimer/Publisher's Note: The statements, opinions and data contained in all publications are solely those of the individual author(s) and contributor(s) and not of MDPI and/or the editor(s). MDPI and/or the editor(s) disclaim responsibility for any injury to people or property resulting from any ideas, methods, instructions or products referred to in the content.